

# Learning Contextual Runtime Monitors for Safe AI-Based Autonomy

Alejandro Luque-Cerpa

luque@chalmers.se

Chalmers University of Technology  
and University of Gothenburg  
Gothenburg, Sweden

Sanjit A. Seshia

Sseshia@berkeley.edu

University of California  
Berkeley, USA

Mengyuan Wang

mengyuan@chalmers.se

Chalmers University of Technology  
and University of Gothenburg  
Gothenburg, Sweden

Devdatt Dubhashi

dubhashi@chalmers.se

Chalmers University of Technology  
and University of Gothenburg  
Gothenburg, Sweden

Emil Carlsson

caremil@chalmers.se

Sleep Cycle AB  
Gothenburg, Sweden

Hazem Torfah

hazemto@chalmers.se

Chalmers University of Technology  
and University of Gothenburg  
Gothenburg, Sweden

## Abstract

We introduce a novel framework for learning context-aware runtime monitors for AI-based control ensembles. Machine-learning (ML) controllers are increasingly deployed in (autonomous) cyber-physical systems because of their ability to solve complex decision-making tasks. However, their accuracy can degrade sharply in unfamiliar environments, creating significant safety concerns. Traditional ensemble methods aim to improve robustness by averaging or voting across multiple controllers, yet this often dilutes the specialized strengths that individual controllers exhibit in different operating contexts. We argue that, rather than blending controller outputs, a monitoring framework should identify and exploit these contextual strengths. In this paper, we reformulate the design of safe AI-based control ensembles as a contextual monitoring problem. A monitor continuously observes the system’s context and selects the controller best suited to the current conditions. To achieve this, we cast monitor learning as a contextual learning task and draw on techniques from contextual multi-armed bandits. Our approach comes with two key benefits: (1) theoretical safety guarantees during controller selection, and (2) improved utilization of controller diversity. We validate our framework in two simulated autonomous driving scenarios, demonstrating significant improvements in both safety and performance compared to non-contextual baselines.

## Keywords

Runtime assurance, Contextual bandits, Safe AI-based autonomy

## 1 INTRODUCTION

Recent advancements in machine learning (ML) have been pivotal to the progress of autonomous cyber-physical systems (ACPS) [5, 21]. ML-based models, such as neural networks, have enabled scalable solutions for complex tasks in perception, planning, and control. Growing reliance on ML-based models introduces significant challenges related to safety [3, 36]. ML models are inherently brittle; unanticipated changes in the ACPS’s environment can degrade performance and lead to faulty outcomes that may compromise system safety. This brittleness arises from various factors, such as the training algorithms used, the model architecture, and the nature of the training data. One common approach to mitigating uncertainty is

through the use of ensembles: multiple models whose predictions are combined to produce a more robust output. While ensemble methods can improve overall accuracy, they often rely on averaging or voting mechanisms that may miss out or even dilute the actual individual strengths of different controllers, especially when each one performs best in distinct operational contexts. As a result, traditional ensemble techniques may reduce variance but fail to exploit contextual specialization among controllers.

In this paper, we reframe the problem of building black-box (AI-based) control ensembles as a contextual monitoring problem. Rather than blending all controller outputs, a monitor identifies and exploits contextual expertise, i.e., based on the current operational context of the ACPS, such as environmental conditions, it determines which controller is safest to deploy. If no controller can be trusted to maintain safety, the monitor, following a Simplex-style strategy, diverts to a fail-safe that guarantees safety at the cost of reduced performance. We provide a formalization of the problem of learning contextual monitors for control ensembles and present a framework for learning such monitors. Starting with a formal specification, defining the safety constraints of an ACPS, our framework enables the learning of contextual monitors that come with formal statistical guarantees on safety.

Consider, for example, the scenario depicted in Figure 1. An autonomous vehicle is equipped with an ensemble of (black-box) image-based controllers for lane keeping. These controllers could be, for example, realized by an ensemble of convolutional neural networks of different architectures and trained on different data sets. Depending on how each CNN was trained and the distribution of its training data, each controller may exhibit specific biases, for instance, due to the presence or absence of particular features during training, or because they were trained on distinct datasets, leading to varying performance across different contexts. So, one controller may perform better in certain weather conditions, another controller may be more robust in certain traffic situations or times of the day. The goal is to manage this ensemble via a monitor that learns to identify which controller is most reliable in a given context, and delegates control accordingly. In the case that the monitor determines that none of the controllers can be trusted to uphold the safety specification in a current context, it triggers a switch to a fail-safe controller, usually realized by a less-optimal but verified control

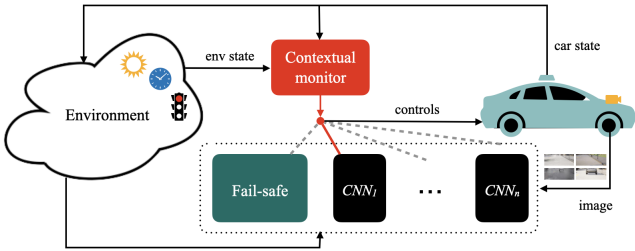


**Figure 1: Autonomous car equipped with a contextual monitor for an ensemble of CNN-based controllers.**

policy, thus ensuring continued safety. A key challenge here will be to create a monitor that maintains safety, yet without being to overly conservative, i.e., that resorts to too many unnecessary switches to the fail-safe.

Our contextual approach enables us to leverage the inherent biases in individual controllers, something that stands in contrast to traditional, ensemble methods such as (weighted) averaging over bagged ensembles, boosting, or mixture-of-experts techniques [32]. While these methods are effective at reducing overall variance, they typically fail to exploit the specific strengths that individual controllers exhibit in particular operational settings. This limitation is best understood by considering an ensemble's behavior relative to the operational domain (OD) of the ACPS. For example, in our earlier scenario, the OD may correspond to the environmental conditions under which the system operates. The goal is to construct ensembles that provide robust coverage of the OD, i.e., ones that can operate safely across most, if not all, contexts within this OD. As illustrated in Figure 2, we identify several possible scenarios along this spectrum. In the ideal case, each controller individually offers broad OD coverage, with only minor weaknesses that can be compensated for by others in the ensemble (the  $\neg B, C$  case). In such situations, conventional ensemble techniques often perform well at improving accuracy. However, this ideal scenario is rarely guaranteed. More commonly, although the ensemble collectively covers the OD, individual controllers exhibit biases toward specific regions (the  $B, C$  case). In such cases, simple averaging may fail to mitigate biases and can even degrade performance. A worse situation occurs when the controllers are biased and, collectively, fail to provide sufficient OD coverage (the  $B, \neg C$  case). In this scenario, our approach can still exploit controller biases to select whichever controller remains safe, if any. The final case ( $\neg B, \neg C$ ) represents a poorly trained ensemble in which all methods, contextual or otherwise, will likely lead to safety violations or degraded performance.

Under this view, the monitor learning problem is thus contextual, one that can be naturally phrased and solved by drawing correspondence with contextual multi-armed bandit problems. Contextual bandits are a variation of the multi-armed bandit problem where rewards associated with the arms change at each round depending on the context [24, 25]. In our setting, the arms represent a set of black-box (ML-based) controllers (e.g., the ensemble of CNN-based controllers from our example above), the context corresponds to the environmental settings in which the system is deployed (e.g., weather, time of day, road features, etc.), sometimes it could also

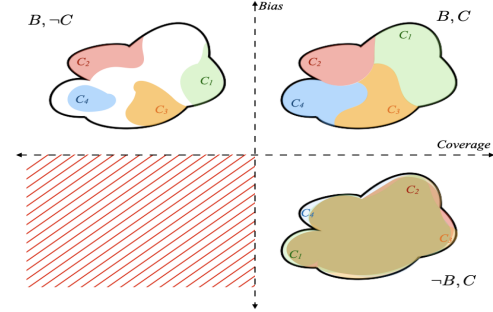


**Figure 2: Operational domain bias-coverage spectrum of ensemble-based control.**

include the system state, and the rewards are determined by the satisfaction of a system-level specification that defines the system's safety requirements (e.g., avoiding lane invasions, keeping a certain distance to other vehicles and objects). The goal is to learn a monitor that optimizes performance while maintaining safety, selecting the most suitable controller for a given context, and relying on the fail-safe controller only when necessary. From a predefined space of possible monitors, our method learns a monitor whose performance matches closely the optimal monitor within that space, with a guaranteed bound on the error [10] quantified in terms of the regret, a standard criterion in bandit literature.

Contextual bandits provide a dynamic and guided approach that allows for continually learn from feedback [6]. Our approach contrasts with the naive approach of simply training a classifier to map a context to a controller. The latter is a purely passive learning approach, whereas bandits allow one to adapt to the dynamic nature of ACPS environments and to continually incorporate feedback to improve the system. Contextual bandits are in the spirit of *reinforcement learning* (RL) and can be seen as a simpler, lightweight version of RL that does not change the state of the system, which is the focus of this paper.

From a practical view, we show that our approach provides significant improvements in performance over methods that use simple, non-contextual approaches. We validate the latter, through a series of experiments, using a case study from the domain of autonomous driving, building on the example above, demonstrating the efficacy of our approach and highlighting further the importance of contextual learning in building control ensembles for ML-based ACPS. Our contributions can be summarized as follows:

- We introduce and formalize the problem of learning contextual runtime monitors for control ensembles
- We present a framework for learning contextual monitors with formal statistical safety guarantees
- We provide a thorough experimental evaluation showing the efficacy of our approach in enhancing safety while maintaining a reasonable degree of performance, specifically showing the benefits over non-contextual methods.

## 2 RELATED WORK

We review key related research, focusing on three areas closely connected to our work: *safety monitoring and shielding*, *ensemble-based control*, and *contextual bandits in decision-making*.

### 2.1 Safety Monitoring and Shielding

The design of runtime monitors has long been, and continues to be, crucial in the development of safe and reliable cyber-physical systems (CPS) [4]. A key application of runtime monitoring is the validation of design assumptions. This has typically followed a specification-based approach, where design assumptions are captured in formal specifications [11, 30] and directly monitored at runtime. In our setting, while we assume access to a general system-level safety specification, we cannot assume that we can synthesize the monitor directly from this specification, as it is defined over a different space, the context space. Thus it must be learned using a data-driven approach with respect to this specification. This also stands in contrast to prominent approaches based on shielding [2]. Such approaches typically assume knowledge of system dynamics (e.g., MDP in shielding) along with a conservative environment model. In contrast, our monitors do not make such assumptions, are defined solely over observable features, and do not assume direct monitorability of the specification. Similar argument holds for methods based on barrier certificates [20] or safety filters [19]. Lastly, there is a series of works that address the problem of predictive safety monitoring, e.g., in RL settings to predict the impact of actions on safety [43], and also those in adversarial settings [29]. Such approaches can be adapted to our settings to predict contexts to include the aspect of predictiveness, but we keep such study for future work. Many works also looked into approaches for safe model-predictive control (MPC) (e.g., [31, 42]). While showing safer outcomes, such approaches again require access to a system dynamics model. A key distinction to the methods above lies in our focus on addressing the aspect of context dependent monitoring and how it can help in enhancing safety while balancing performance.

### 2.2 Ensemble-based Control

Ensemble-based control is a widely used technique in control systems, machine learning, and robotics, where multiple controllers (or models) are combined to make decisions or control actions [27, 33, 39, 41]. Such ensembles improve robustness by reducing the impact of individual controller errors. Most ensemble-based control methods rely on averaging approaches to smooth out these errors. For example, Ramakrishna et al. demonstrate how adapting weighted control ensembles within a Simplex architecture can improve system performance [33]. Li et al. show that ensembles of DNN regressors can better account for uncertainty in adaptive cruise control settings [27]. Tong et al. illustrate how ensembles can reduce error bounds in deep model predictive control [39]. Some contextual extensions of weighted averaging have been explored through mixture-of-experts frameworks [32], where a learning-enabled model, such as a neural network, is trained to determine the contribution of each controller based on the observed context. In these approaches, controller outputs are aggregated dynamically according to the weights computed by the model. In contrast, our approach leverages the strengths of

each controller without diluting them through aggregation, allowing the system to exploit individual expertise more effectively.

### 2.3 Contextual Bandits in Decision-Making

Contextual bandits are a classical topic in the bandit literature [24, 25]. The logistic bandit setting has received much attention recently in the binary case [14, 15], see also [7] for an application to learning preference orderings. The contextual multiarm bandit model framework has attracted a lot of attention in various applications, from recommender systems and information retrieval to healthcare and finance, because of its stellar practical performance in learning from feedback combined with attractive theoretical properties. See [6] for a survey of applications. However, we are not aware of any applications in the domain of interest in this paper.

## 3 PROBLEM FORMULATION

In this section, we formally define the problem of learning contextual monitors. The problem is defined over three main ingredients: *monitor-guided systems*, *safety specifications*, and *contexts*. The learning problem is then one where we want to learn a monitor that when plugged in into the monitor-guided systems, will, for any given context, choose a controller that is trusted to maintain the safety specification, up to some statistical boundaries, and decides to switch to fail-safe if no controller is trusted to be used safely.

We start by formally introducing the notion of monitor-guided systems, and with it the definitions for safety specification and contexts.

**Notation** If  $V$  is a set of variables that are defined over domain  $\mathbb{D}$ , we define a valuation of  $V$  as a function  $v: V \rightarrow \mathbb{D}$ , and write the set of valuations of  $V$  as  $\mathbb{D}^V$ . For a set  $A \subseteq V$ , we define  $v_A: A \rightarrow \mathbb{D}$  as the valuation resulting from restricting  $v$  to the variables in  $A$ . Lastly, we use  $Z^*$  to refer to the set of finite sequences over elements of a set  $Z$ , also referred to by the traces over  $Z$ .

### 3.1 Monitor-Guided Systems

An abstract view of the architecture of systems studied in our paper is depicted in Figure 3. The system is composed of an environment and a controlled entity. This entity is controlled by a set of controllers  $c_1, \dots, c_n$ , which in turn are managed by a monitor. The controls computed by a controller determine how the state of the controlled entity changes. The role of the monitor is to dynamically adapt the controls of the most safe controller at each execution step based on a current observed context. The context can be defined in terms of the state of the controlled entity and that of the environment (or a part thereof). In the rest of the paper we will denote the architecture in Figure 3 by a *monitor-guided systems (MGS)*.

Formally, an MGS is a tuple  $\mathcal{S} = (V_{env}, V_{state}, V_{cont}, C, \iota, \pi)$ . The set  $V_{env}$  is a set of environment variables over which we define a state of the environment. The set  $V_{state}$  is a set of variables over which we define a state of the controlled entity. The set  $V_{cont} \subseteq V_{state} \cup V_{env}$  is a set of context variables. Usually context variables are associated with current sensor measurements or state of the plant. W.l.o.g., we assume all variables are defined over the same domain  $\mathbb{D}$ . The set  $C$  is a set of controllers, where  $c \in C$  implements a function  $c: (\mathbb{D}^{V_{state} \cup V_{env}})^* \rightarrow \mathbb{D}^{V_{state}}$ . The state  $\iota \in \mathbb{D}^{V_{state}}$  is the initial system

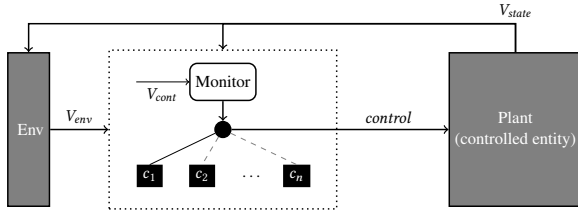


**Figure 3: A general view of a monitor-guided system consisting of  $n$  controllers managed by a contextual monitor.**

state. Lastly,  $\pi: \mathbb{D}^{V_{cont}} \rightarrow C$  is a monitoring policy that for a context  $\xi \in \mathbb{D}^{V_{cont}}$  returns a controller  $c \in C$ .

**REMARK 1.** We note that in this paper, we consider MGS defined in terms of positional contexts, i.e., the output of a monitor depends only on the current context. Such contexts are common in ACPS, e.g., operational domains [35] are usually defined in terms of current environmental conditions, constellation of traffic, etc. Our results show that the positional setting studied provides rich theoretical insights and highlights key challenges, giving a foundation for more state-based settings. We note, though, that, typically, monitors in CPS operate over a bounded history, which then can be reduced to the positional setting. The study of state-full contexts is left for future work.

A MGS thus follows the concept of the well-known Simplex architecture [37], where a decision module is used at runtime to choose between an optimal, yet not necessarily verified controller (in our case between several optimal controllers), and a verified safe controller. Assuming one of the controllers in an MGS is a verified safe-controller, the policy plays the role of a decision module, but one that based on a certain context defined in terms of environment features and system state decides which controller out of many optimal controllers should be used to control the system, before deciding to switch to the safe controller.

**Specifications.** We define the semantics of an MGS  $\mathcal{S}$  by its set of executions traces  $Traces(\mathcal{S}) = \{\tau^1 \dots \tau^k \in (\mathbb{D}^{V_{state} \cup V_{env}})^* \mid \tau^1_{V_{state}} = \iota \text{ and } \forall 1 < i \leq k. \tau^i_{V_{state}} = \pi(\tau^{i-1}_{V_{cont}})(\tau^1_{V_{state}} \dots \tau^{i-1}_{V_{state}})\}$ . We define the safety of a system in terms of finite trace specifications [16], i.e., a set of finite traces from which the system traces should not deviate. A specification is thus a set  $\varphi \subseteq (\mathbb{D}^{V_{state} \cup V_{env}})^*$ . We say that a trace  $\tau \in Traces(\mathcal{S})$  satisfies  $\varphi$ , denoted  $\tau \models \varphi$  if and only if  $\tau \in \varphi$ . We further say, that  $\mathcal{S}$  satisfies  $\varphi$ , denoted  $\mathcal{S} \models \varphi$ , if  $\forall \tau \in Traces(\mathcal{S}). \tau \models \varphi$ .

Putting all concepts together, an example of a safety specification in the scenario of the autonomous car in Figure 1 could be an invariant requiring that there are no lane invasions, and that the car should always keep a certain distance to other objects on the road. A contextual monitor will now have to decide based on an observed context, e.g., weather condition, which controller is safest, in terms of satisfying the specification above.

Several formalisms exist in the literature to describe finite trace specification (e.g., logics like STL [28], automata [16]). Our approach is agnostic to any specification formalism, as long as specifications are monitorable.

### 3.2 Problem Statement

Using the concepts above, our contextual monitor learning problem can now be defined as follows. Let  $\mathcal{S} = (V_{env}, V_{state}, V_{cont}, C, \iota, ?)$  be an MGS with a missing monitoring policy, and with  $V_{state}$  and  $V_{env}$ , defined over a domain  $\mathbb{D}$ . Let further a specification  $\varphi \subseteq (\mathbb{D}^{V_{state} \cup V_{env}})^*$ , and  $\Pi$  be a set of policies from  $\mathbb{D}^{V_{cont}} \rightarrow C$ . Our goal is to compute a policy  $\pi \in \Pi$  that given a context  $\xi \in \mathbb{D}^{V_{cont}}$  selects a controller  $\pi(\xi)$  so it approximates an optimal policy  $\pi^*$ . The optimality is measured in terms of the following *regret* [25]:

$$\max_{\xi \in \mathbb{D}^{V_{cont}}} L_{\mathcal{S}}(\pi(\xi), \varphi) - L_{\mathcal{S}}(\pi^*(\xi), \varphi)$$

where  $L_{\mathcal{S}}(\pi(\xi), \varphi) := \Pr(\mathcal{S}[\pi] \not\models \varphi \mid \xi)$

with  $\mathcal{S}[\pi]$  defining the MGS resulting from replacing  $?$  with  $\pi$  in  $\mathcal{S}$ . The regret is thus the maximal difference between the loss suffered by the optimal controller and the loss of the controller computed by our policy  $\pi$  maximized over all contexts. Our goal is to minimize this regret. In the next section, we present an algorithm that learns a monitoring policy with bounds on this regret (Theorem 4.1).

## 4 LEARNING CONTEXTUAL MONITORS

Our learning problem is inherently a contextual one, and can be naturally approached by drawing on techniques from the contextual bandit literature [25]. It is this choice that enables us to obtain formal regret-minimization bounds as we show later in this section.

We restrict ourselves to monitors that model a violation probability using logistic regression [1]. That is, given a controller  $c$  and context  $\xi$ , we assume that there is some unknown vector  $\theta_c$  such that the probability that  $c$  violates the specification, given  $\xi$ , can be written as  $\Pr(Y = 1|c, \xi) = \sigma(\theta_c^\top \xi)$  where  $\sigma(\cdot)$  is the logistic function, and  $Y$  is a Bernoulli variable representing whether a violation has occurred. We also restrict ourselves to bounded monitors and bounded contexts, technical assumptions which are standard in the bandit literature, see ([10] and references therein).

Following the logistic regression model, we can then rewrite the regret as defined in our problem statement to:

$$\max_{\xi \in \mathbb{D}^{V_{cont}}} |\sigma(\theta_{\pi(\xi)}^\top \xi) - \sigma(\theta_{\pi^*(\xi)}^\top \xi)|$$

where  $\pi(\xi) \in \operatorname{argmin}_{c \in C} \sigma(\theta_c^\top \xi)$

Learning an optimal policy  $\pi$  thus resorts to solving the minimization problem above for the vectors  $\{\theta_c\}_{c \in C}$ . In the following, we define a matrix  $\theta$  whose rows are the vectors  $\theta_c$ , and we describe a learning approach based on contextual bandits to learn this matrix. This overall process is shown in Algorithm 1. In our setting, a learner interacts with the system over a sequence of  $T$  rounds. At each round  $t$ , the learner selects a context  $\xi$  and a controller  $C_t$ , and runs this controller on the system in that context. Before moving on to the next round, the learner observes the outcome  $Y_t$ . In our setting,  $Y_t$  is a binary variable that tells whether the system using the chosen controller violated the safety specifications  $\varphi$ . At the end of each iteration  $t$ , the row  $\theta_c$  of the matrix  $\theta$  is updated with the values  $\theta_{t,c}$ , which are computed for a selected controller  $c$  as the

maximum-likelihood estimate (MLE):

$$\theta_{t,c} \in \underset{\theta'_c \in \mathbb{R}^{|V_{\text{cont}}|}}{\operatorname{argmax}} \sum_{j=1}^t \mathbb{1}_{(C_j=c)} \left( Y_j \log \sigma(\theta_c'^\top \xi_j) + (1 - Y_j) \log(1 - \sigma(\theta_c'^\top \xi_j)) \right)$$

After  $T$  rounds, the learner outputs a monitor  $\pi_T$  corresponding to the matrix  $\theta$ , whose rows are the vectors  $\theta_{T,c_1}, \dots, \theta_{T,c_{|C|}}$ . In the following, we provide details about the individual steps.

**Select context and controller (Line 3).** The key component of our approach is how to decide which controller to test over what context during the learning phase. We do this using the value of an uncertainty metric based on the Hessian of the negative log-likelihood:

$$H_t(\theta_{c,t}) = \sum_{s=1}^t \mathbf{I}_{(C_s=c)} \dot{\sigma}(\theta_{c,t}^\top \xi_s) \xi_s \xi_s^\top$$

Intuitively, the Hessian indicates the curvature while moving in a particular direction. A higher curvature indicates more sensitivity to changes in that direction, which is linked to more uncertainty because small changes lead to unpredictable results. This notion of uncertainty is inspired by work done on logistic bandits [13, 15, 23]. The technical details can be found in the appendix.

Choosing a controller in a round can be done in many ways. A prominent way is to randomly sample a context, according to a given distribution, and then choose the controller with the highest uncertainty. Another method that provides better theoretical upper bounds on regret, and which we show to be effective in our experiments, is to choose the controller with the highest uncertainty over all contexts. In Theorem 4.1, we show the order of these bounds. This is an adaptation of the sampling rule of [10] to our setting.

At a high level, the computation in round  $t$  can be done using the current MLE values  $\theta_{t,c}$  for each controller  $c$  and the corresponding Hessian of the negative log-likelihood to measure the epistemic uncertainty about a controller's safety in a given context. Since initially we do not have information about the values  $\theta_{t,c}$ , the implementation runs the system once with each controller in a random context before using the uncertainty values. We leave the complete mathematical formulation to the appendix.

**Evaluate a controller (Line 4).** A selected controller  $C_t$  is evaluated over a context  $\xi_t$ , w.r.t. the specification  $\varphi$ , by running the system with  $C_t$  and computing  $Y_t$ , indicating whether the specification was violated or not. The latter can be computed by using any trace checking algorithm for  $\varphi$ .

**Update monitor and uncertainty of controllers (Line 6).** The monitor is retrained over a new set  $\mathcal{D}_t$  that expands on  $\mathcal{D}_{t-1}$  with new data collected during evaluating the controller (Line 4). The uncertainty update can be performed using the Sherman-Morrison formula (Sherman and Morrison 1950). A full mathematical walk through is kept to the appendix due to space limits.

By applying Algorithm 1 for a sufficient number of iterations we obtain a monitor that closely approximates the optimal monitor. Formally, we have the following result, which upper bounds the regret by a quantity that quickly decreases to 0 with the number of rounds. The proof in detail is given in the appendix.

---

#### Algorithm 1 Contextual monitor learning

---

**Require:** Bandit algorithm **Alg**, specification  $\varphi$ .

- 1: Initial empty dataset  $\mathcal{D}_0 = \{\}$
- 2: **for**  $t=1, \dots, T$  **do**
- 3:    $\xi_t, C_t = \text{Alg}.\text{select}(\mathcal{D}_t)$ .
- 4:    $Y_t = \text{run}(C_t, \xi_t, \varphi)$ .
- 5:    $\mathcal{D}_t := \mathcal{D}_{t-1} \cup \{(\xi_t, C_t, Y_t)\}$ .
- 6:    $\pi_t = \text{Alg}.\text{update}(\mathcal{D}_t)$ .
- 7: **end for**
- 8: **return**  $\pi_T$

---

**THEOREM 4.1.** *Using Algorithm 1, selecting the controller and context with the highest uncertainty, we have that the regret is bounded by  $O(\sqrt{\log(T)^2/T})$ .*

**REMARK 2.** *The assumption that the probability of failure can be described as a logistic model in the context is common in the multi-armed bandit literature [14, 26] and the active learning community [10]. This assumption allows us to derive efficient sampling rules. While it might seem restricted at first glance, we want to highlight that we do not make any assumptions about how the context vector  $\xi$  is generated. In fact, our approach can be built on top of any non-linear feature extractor, for example a neural network, and performing the exploration in the last layer using our approach. This is common practice in the bandit literature [34, 40].*

**REMARK 3.** *The reasons to sample contexts considering the uncertainty in Alg. 1 is to deal with the problem of having a lower bound on the suboptimality gap. This arises when the number of rounds  $T$  is much lower than the number of contexts  $|\mathbb{D}^{V_{\text{cont}}}|$  (see [10] for details).*

## 5 EXPERIMENTAL EVALUATION

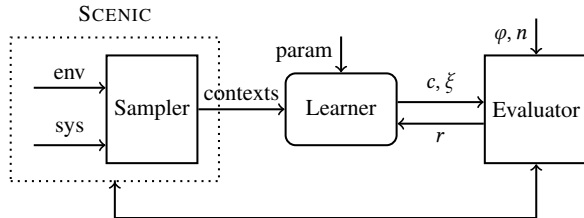
We assess the efficacy of our proposed approach by investigating the following research questions:

- **RQ1: Sanity check.** Does a monitor learned using our approach indeed select the controller best for a context?
- **RQ2: Comparing to other baselines.** How does our approach compare to other ensemble methods, like common weighted average and mixture-of-experts methods?
- **RQ3: Active bandits vs passive learning.** Does our active learning approach result in more accurate monitors than simple one-shot passive learning approaches?
- **RQ4: Simplex vs multi-Simplex.** What is the impact of larger control ensembles on the accuracy of monitors?

We address these questions by evaluating our approach on two scenarios in autonomous driving. We first describe the experimental setup, including details about implementation and scenarios, and then present our results and findings.

### 5.1 Framework and Implementation

The workflow of our prototypical implementation is shown below.



The *Learner* implements the main loop in Algorithm 1. The parameters of the learner include the set of controllers  $C$ , the total number of rounds  $T$ , and the number of rounds  $e$  the Learner collects data in before retraining the monitor. While Algorithm 1 chooses in each iteration the context  $\xi$  and the controller  $c$  with the highest uncertainty. In practice, to avoid computation overhead, we sample a large number of contexts. Then, the learner chooses the context and controller with the highest uncertainty. Sampling the contexts and computing the reward is done with the help of the Sampler and Evaluator, respectively.

The *Sampler* has access to a system model. In our implementation, we realize the modeling and sampling using the scenario description language SCENIC [18]. A scenic program in our setting will define a distribution over the context space. Using SCENIC, we generate random scenarios in which we simulate our system. Each sampled scenario defines a unique context. Once a context  $\xi$  and  $c$  are selected, they are forwarded by the Learner for evaluation.

The *Evaluator* then runs the system in  $\xi$  using  $c$  and evaluates the execution to obtain a (binary) reward  $r$ . The reward is determined by validating the satisfaction of a safety specification  $\varphi$  in a simulation of  $n$  steps. The learner uses the reward to update the training data and, in turn, learns a new model. In our setup, the evaluator is also realized using the Scenic execution engine.

## 5.2 Scenarios

Our scenarios were inspired by real-world problems of how to safely deploy vision-based models for autonomous steering and collision avoidance [8, 9, 17]. Our scenarios are simulated using the open source high-fidelity CARLA simulator [12]. We use SCENIC’s interface to CARLA to generate random scenarios by sampling from the context space. In the following, we provide details for our two scenarios, particularly the controllers, context space, and specification used. Figures 4 and 5 show sample instances for both scenarios.

**5.2.1 Scenario 1: Autonomous steering.** An autonomous car is driving in a city. The car is equipped with a set of controllers that compute the steering angle of the car based on images received from a camera. Each controller is composed of a CNN that computes the cross-track error (CTE) to the centerline of the lane, and a PID controller that uses the CTE to compute the steering angle. Additionally, the car is equipped with a fail-safe controller that can guide the car slowly and safely through the city, based on the internal follow-lane behavior of Carla.

**CNN-based controllers.** To generate training data for the controllers, we ran simulations for each of the 14 weather presets with another car positioned at a random distance ahead of the ego car. We collected images from simulations using a camera installed in the front of the car. Each image was associated with the CTE value. We collected  $\sim 90K$  data instances to train each controller.

**Specification.** We focus on the ability to perform lane keeping. The safety specification used is thus one that requires the at no time for the car to leave its lane for more than 30 simulation steps.

**Contexts.** We assume the presence of another car. The context space is defined over the following features, which can change: the weather, the time of the day, road features such as being on a straight road or at an intersection, and the distance to the other cars ahead. Each context in our scenario is thus represented by a tuple  $(w, t, i, d)$ , where  $w$  represents the weather,  $t$  the time of day,  $i$  the road type, and  $d$  the distance to the vehicle ahead if present. For weather and time of day, we use one of the 14 weather-time configurations predefined in CARLA. The road type  $i$  is a binary value 0 or 1, indicating whether the car is at an intersection ( $i = 1$ ) or not ( $i = 0$ ). The distance  $d$  is a real number s.t.  $d \in (0, 50] \cup \{100\}$ . If the other vehicle is not present, or if  $d > 50$ , we assume that the vehicle ahead is too far away to consider it part of the context ( $d = 100$ ). Note that, while  $w$  and  $t$  are fixed for each simulation,  $i$  and  $d$  can change depending on the movement of both vehicles. In our experiments, we discretize the distance  $d$  into 5 clusters, so we explore a set of 140 different contexts when we apply Algorithm 1. In Figure 4, we can observe instances of these contexts.

**5.2.2 Scenario 2: Dynamic urban environment.** This scenario focuses mainly on testing the collision avoidance ability in a dynamic urban environment, as illustrated in Figure 5. In this case, the scenario involves interactions with other agents on the road, including pedestrians and other vehicles. The controllers are CNNs that compute the CTE to provide it to a PID controller, but that also compute the target speed that the car should reach. The target speed is provided to the PID controller to determine the corresponding throttle or braking intensity. The car is also equipped with a fail-safe controller, but it also brakes if the distance to another car or pedestrian ahead is lower than a given threshold.

**CNN-based controller.** Similar to Scenario 1, we ran simulations for each of the 14 weather presets with other cars or pedestrians positioned at a random distance ahead of the ego car. The training images were also taken from simulations. Each image was associated with the CTE value and the current speed. We collected  $\sim 90K$  data instances to train each controller.

**Specification.** We focus on the ability to perform lane keeping and avoid collisions. The safety specification used is thus one that requires at no time for the car to crash or to leave its lane for more than 30 simulation steps.

**Contexts.** Each context is represented by a tuple  $(w, t, i, d_c, d_p)$ , where  $w$  represents the weather,  $t$  the time of day, and  $i$  the road type as same as defined in Scenario 1: Autonomous steering. The variable  $d_c$  represents the distance to the nearest visible vehicle if present, while  $d_p$  represents the distance to the nearest visible pedestrian if present. Again,  $w$  and  $t$  are fixed for each simulation, while  $i$ ,  $d_c$ ,  $d_p$  can change depending on the movement of the agents in the simulation. After discretizing  $d_c$  and  $d_p$  in 5 clusters each, we have a total of 700 contexts to explore.

*The algorithm is implemented in Python, and all the experiments were conducted on a machine with 2.9 GHz 32-Core CPU, 576GB of RAM, and an NVIDIA Tesla T4 GPU.*



Figure 4: Three instances of Scenario 1, with different weather conditions, distance between cars, and road types.



Figure 5: Three instances of Scenario 2, with different weather conditions, and different pedestrians and cars configurations.

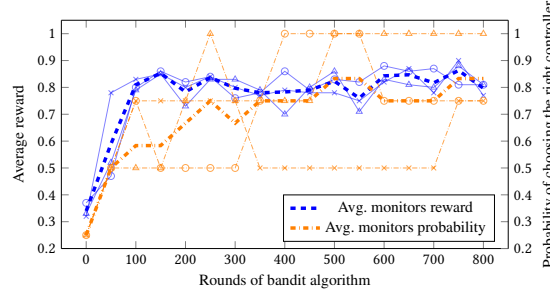


Figure 6: Results for RQ1: Sanity Check.

### 5.3 RQ1: Sanity check

For this experiment, we take 4 biased controllers from Scenario 1. One controller is trained on contexts  $\xi_1 = (w, t, i, d)$  where the car ahead is close, ( $d \in [5, 10]$ ) and the weather/time ( $w, t$ ) is given by the Carla preset *ClearNoon*. The other three controllers are trained on contexts without another car ahead,  $\xi_2 = (w, t, i, 100)$ , and with weather/time contexts ( $w, t$ ) from  $W = \{\text{ClearSunset}, \text{HardRainNoon}, \text{HardRainSunset}\}$ , respectively. In our learning process, we train the monitor only in contexts of form  $\xi_1$  or  $\xi_2$ . After learning, we run a series of random simulations, but also exclusively on instances coherent to  $\xi_1$  or  $\xi_2$ . In each simulation, we check if the monitor chooses the expected controller  $c_\xi$  when observing a context  $\xi$ . We used our approach to train three monitors. The hyperparameters chosen were  $T = 800$  (total number of rounds),  $e = 25$  (number of rounds the Learner collects data in before retraining the monitor), and  $n = 300$  (number of simulation steps, see also Section 5). The monitors were evaluated over 100 simulations every 50 rounds.

The results are presented in Figure 6. In the initial learning rounds, the monitor chooses a controller randomly, so we expect the initial average reward (average satisfaction of the specification) to be low. With each round, the average reward grows. It stabilizes after around 200 iterations with rewards around 0.8 (solid, blue lines). We also

compare the performance of the monitors against the true probability of the bandit algorithm selecting the correct controller for each context (orange, dashed lines). Note that the observed probabilities may sometimes be lower compared to the higher quality of the monitors. For example, for one monitor, the probability was 0.75. A deeper analysis revealed that the algorithm correctly identified the expected controllers for highly distinguishable contexts of *ClearNoon* (with a car close) and *ClearSunset*. However, for the contexts of *HardRainNoon* and *HardRainSunset*, which are highly similar, the corresponding controllers performed with nearly equal quality. As a result, the bandit algorithm may not consistently differentiate between them, and the probability of choosing the right controller varies in our experiment between 0.5 - 1.0. Consequently, a limitation arises: identifying contexts and learning from them highly depends on the expressiveness of the available observable features. We conclude that our approach successfully learns to select a suitable controller for the right context if such a controller is available. If not, a switch to the fail-safe will be triggered.

### 5.4 RQ2: Comparing to other baselines

In this experiment, we compare our contextual approach to other ensemble-based techniques commonly used in ensemble-based control. In regression tasks, like in our scenarios, common ensemble techniques are based on (weighted) averaging methods. This could be simple approaches based on bagging, or one that allows for contextual information to be used in order to dynamically compute the weights, such as mixture-of-experts methods [32]. Our comparison is performed over all three settings described in Figure 2. We especially show that, depending on the setting, our contextual approach has a significant impact on the common ensemble approaches, especially for scenarios with more complex dynamics, such as Scenario 2. We specifically perform the comparison for two types of monitors, one based on logistic regression as described in the paper, and one where the monitor is implemented by a neural network. The goal here is to specifically show that logistic regressions, in addition to their value in providing theoretical bounds on the regret, indeed provide better generalizations compared to neural networks provided with the same

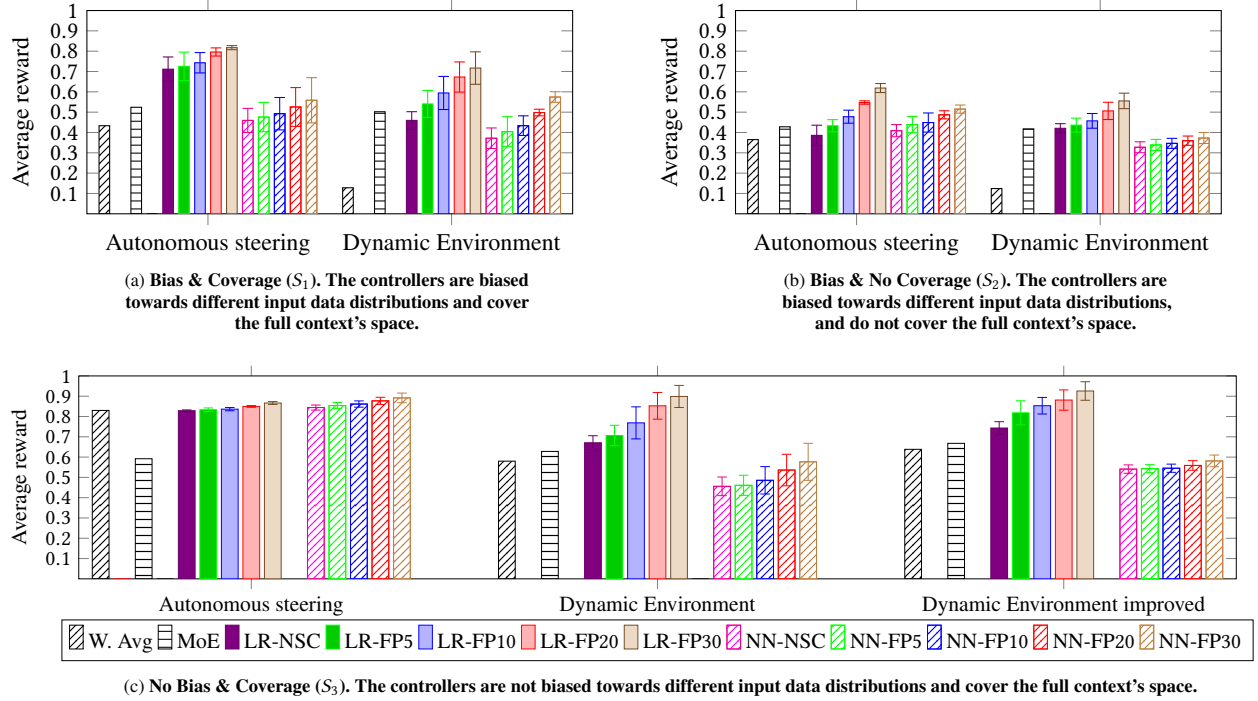


**Figure 7: Results for RQ2: Comparing to other baselines. Weighted Average and MoE) vs two types of monitors: Logistic Regression (LR, filled colored bars) and Neural Network (NN, striped colored bars). The legend key NSC stands for No Safe Controller, FP represents the tolerance rate of False Positive in Percentage, e.g., FP5 stands for a 5% tolerance of FP.**

amount of data. We trained three monitors per scenario and model type (LR, NN). The hyperparameters chosen were  $T = 1000$ ,  $e = 25$ , and  $n = 300$  in each case, and each method is evaluated over 500 simulations.

Independent of the scenario and the setting, we expect the monitors to switch to a safe controller when they do not trust the best controller for a given context. Specifically, we define a confidence threshold  $\varepsilon$  such that, if a monitor returns a controller  $c$  for a context  $\xi$ , and the monitor estimates that the confidence of  $c$  satisfying the specifications is less than  $1 - \varepsilon$ , then the monitor will switch to the safe controller. Increasing the confidence threshold will lead to safer systems, but also to an increase in false positives, that is, cases where the monitor unnecessarily switches to the safe controller.

Our results are given in Figures 7a to 7c. We first describe the setups for our baselines and then present our findings.

*Bagging* The bagging method used computes the weighted average of the output. To estimate the weights, we generated sets of data with  $\sim 450K$  instances, computed the MSE of each controller over that dataset, and then defined the weights as the inverse of the MSE values.

*Mixture of experts.* We compare to an MoE approach based on [32]. A neural network with a gate layer chooses the contribution of each controller to the final decision based on contextual input. We use the same datasets from Bagging to train the MoE models.

*Setting  $S_1$ : Bias & Coverage.* In setting  $S_1$ , the controllers are biased towards different input data distributions and cover the full

context's space. For each scenario, we employ 15 controllers trained on 15 biased datasets generated from different contexts (details in the appendix). The monitors are tested over 500 simulations generated based on the 15 contexts chosen to train the (biased) controllers. Note that, during these simulations, the context can change as explained in Section 5.2, and the monitors may switch to another controller. Specifically, the context variable  $d$  can change for Scenario 1, the context variables  $d_c$  and  $d_p$  can change for Scenario 2, and the variable  $i$  can change for both at each time step.

The results of both scenarios for LR and the averaging ensemble align with our expectations (Figure 7a). Because the controllers are highly biased towards a different context each, the averaging ensemble does not perform well, violating the safety specification in more than half of the simulations for Scenario 1, and in almost 90% of them for Scenario 2. However, our monitors learn to assign the best controller to each context, improving the reward by around 30% in comparison to the averaging ensemble, even when the safety controller is not used. Tolerating rates of False Positives of 5%, 10%, 20%, and 30%, we can observe that the reward increases even further, to a maximum of 80% in Scenario 1, and 70% in Scenario 2.

For NN-based monitors, the results show lower performance than for LR-based monitors. This may indicate that NNs require more data to achieve similar performance. In any case, even if enough data is collected, the statistical guarantees provided by Theorem 4.1 are not guaranteed for NN-based monitors.

*Setting  $S_2$ : Bias & No Coverage* In  $S_2$ , the controllers are also biased, but do not cover the full context's space, which allows us

to introduce out-of-distribution input data. We employ the same 15 controllers used in each scenario for setting  $S_1$ , but we train and evaluate the monitors on the full context's spaces defined for each scenario in Section 5.2.

Because the controllers do not cover the context space, and there are many out-of-distribution data instances, all approaches violate the safety specification for more than half of the simulations (Figure 7b). It is worth noting that, without using the safe controller, MoE is slightly better than LR for Scenario 1 and as good as LR for Scenario 2. However, because we have access to the confidence of the monitors, we can increase the confidence threshold to use the safe controller. With just 5% of false positives, the LR-based monitors already perform better than MoE, and we could raise the reward by up to 30% for Scenario 1 and 20% for Scenario 2 when the rate of false positives grows to 30%.

Again, the results show lower performance for NN-based monitors than for LR-based monitors, as observed in  $S_1$ .

*Setting  $S_3$ : No Bias & Coverage* The controllers are not biased, and they cover the full context's space. For each scenario, we employ 15 biased controllers trained on data collected from i.i.d. sampled simulations from all contexts defined in Section 5.2.

For Scenario 1, because the controllers are well-trained on datasets that cover the full context's space, the safety specification satisfaction is high for the LR and NN monitors. Indeed, even if the monitor does not choose the best controller, the performance is still high. In addition, because the controllers are "not" biased, the reward is also high for the averaging ensemble. For these reasons, our monitors do not find significant differences between the controllers, so the performance of our monitors is slightly worse than the averaging ensemble when the safe controller is not used (FP 0%). However, if we tolerate a rate of false positives of 10% or higher, the monitors perform slightly better than the averaging ensemble. The latter indicates that our approach can exploit even the smallest biases in controllers, although if the context's space is more complex, this may require additional rounds of our algorithm.

Surprisingly, MoE performs much worse than the rest (Section 5.2). This may be due to overfitting or require fine-tuning some hyperparameters. This fact highlights the necessity for approaches that rely on theoretical statistical guarantees like ours.

For Scenario 2, we noticed that the results obtained were worse than for Scenario 1 (Figure 7c). Our main hypothesis was that, because the Dynamic urban environment task (Scenario 2) was much more complex than the Autonomous steering one (Scenario 1), the controllers required more training to achieve similar performance. To test this hypothesis, we trained another set of 15 controllers over datasets of ~150K instances each. Certainly, we can observe that all methods perform better on the new set of controllers (Dynamic Environment improved, Figure 7c). We can also observe that, although the controllers are trained on data collected from i.i.d. sampled simulations from all contexts, the LR and NN monitors achieve better performance than the averaging ensemble and MoE, which implies that they can exploit some biases that appeared during training.

*Conclusion* We have shown the efficacy of our monitors in situations where there is a contextual bias ( $S_1$ , and  $S_3$ : Scenario 2). Furthermore, when the controllers are not trained over the whole OD, and OoD data is introduced ( $S_2$ ), the controller chosen by the

monitor will have a low confidence value, which could prompt the monitor to switch to the fail-safe to reduce risks. Moreover, when "no" bias is present, and the controllers cover the whole context's space ( $S_3$ : Scenario 1), we observed that the non-contextual ensemble and our approach are almost equivalent if the fail-safe is not used. However, our monitors still have access to the safe controller, and the users can now adapt the confidence threshold to make the monitors more or less conservative. Finally, although contextual approaches like MoE can obtain similar or better performance than our monitors in certain situations ( $S_2$ ), fine-tuning may be required, and no statistical guarantees are provided. Lastly, we also experimented with boosting settings. We refer the reader to this case in the appendix. Boosting resulted in even worse performance. Similarly, using NN-based monitors could require more simulations to achieve high performance, and they don't offer statistical guarantees. The next experiment shows the efficacy of using active bandits in comparison to passive learning to learn NN-based monitors.

## 5.5 RQ3: Active bandits vs passive learning

In this section, we compare the efficacy of monitors trained using two distinct data collection strategies: passive learning and active learning. We evaluated both approaches on Setting 3 for both Scenario 1 and Scenario 2, using the same hyperparameters as in RQ2. For each resulting monitor, we ran 500 simulations and plotted the average reward and the tolerance rate of FP against the confidence threshold  $1 - \epsilon$ .

The passive learning approach trains an NN monitor on a dataset generated through random sampling (henceforth Passive NN). Specifically, we generate random contexts and pair them with randomly selected controllers. The corresponding reward for each (context, controller) pair is observed, and these tuples form the training data.

In contrast, the active learning approach employs an LR model as an active query strategy to guide data collection. This LR model identifies (context, controller) pairs that yield the highest uncertainty. Instead of random selection, we prioritize querying these informative samples to obtain their rewards, hence building the training set. An NN monitor (henceforth Active NN) is then trained on this actively-collected dataset. For a comprehensive comparison, we also evaluated the performance of our LR-based monitor (active LR). The "Active LR" thus serves as both the uncertainty-sampling mechanism and a monitor baseline. Note that a passive LR is therefore not included, as it would be conceptually redundant.

To ensure a fair comparison, the passive NN and active NN utilize identical architecture and hyperparameters, and are trained over the same total amount of training data.

The comparison results are shown in Figure 8. For Scenario 1 (Autonomous steering), the task appears relatively simple (Figure 8a), and the passive NN and active NN monitors exhibit nearly identical performance. This suggests that informative, high-uncertainty data points are common enough that a passive approach is sufficient to learn an effective monitor. The extra effort of active sampling yields no significant additional benefit, as these samples are already well-represented in the random data. However, when compared to the Active LR, which gains similar rewards but maintains a much lower tolerance rate of FP, the results indicate that the LR-based

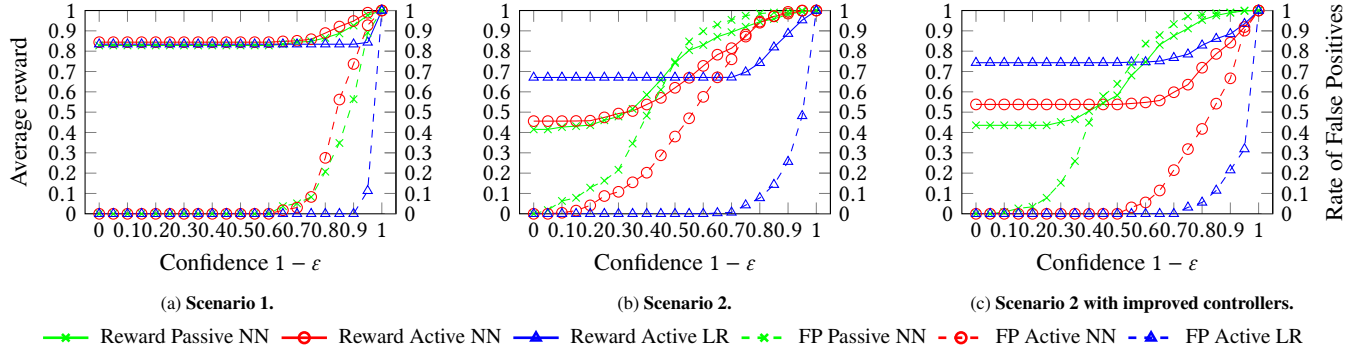


Figure 8: Results for RQ3: Comparison of passive vs. active learned monitors across different scenarios.

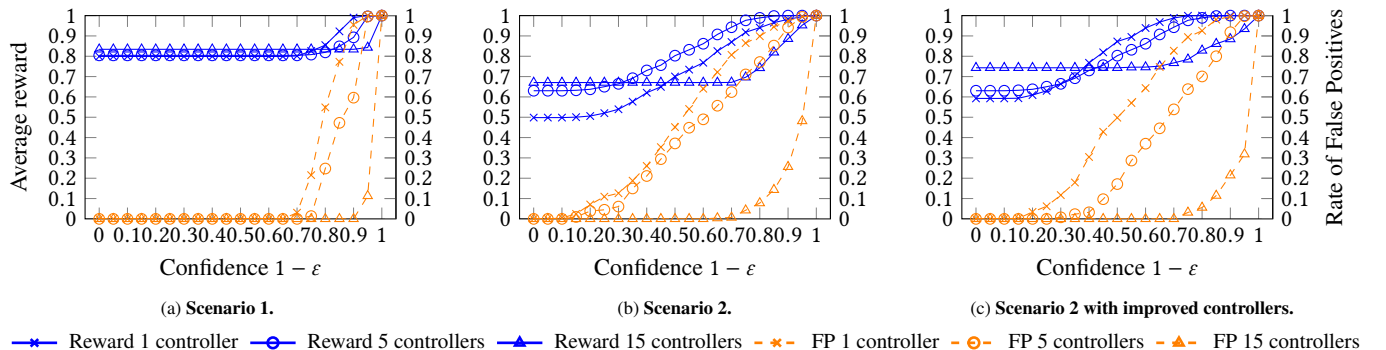


Figure 9: Results for RQ4: Simplex vs. multi-Simplex.

monitor performs as well as the complex NN architecture without extra hyperparameter tuning, while providing statistical guarantees.

The results for Scenario 2 (Dynamic Environment) further reveal the impact of the data-sampling strategy (Figure 8b):

**Active LR vs Active NN.** The Active LR achieves the highest rewards initially and maintains consistent performance across all confidence levels. Conversely, the active NN starts with relatively low rewards, but as the confidence threshold requirement increases, the monitor becomes less certain regarding the optimal controller and triggers the safety backup, causing the FP to increase as well. Notably, even when the rewards of passive NN eventually exceed those of the Active LR (when the tolerance of the confidence threshold is nearly 55%), the Active LR's FP remains at 0%, while the Passive NN's FP already reaches around 47%.

**Active NN vs Passive NN.** Both NN monitors achieve similar rewards at the outset, with the Active NN performing slightly better. As the confidence threshold approaches 30%, it is evident that the Passive NN starts to gain more rewards. However, this correlates with a sharp spike in its FP. In contrast, the Active NN maintains a much lower FP. This suggests that active learning produces a "smarter" and "less conservative" monitor. The active NN learns a more accurate decision boundary, allowing it to trust the "right controller" more often, whereas the Passive NN conservatively triggers unnecessary safety fallback to ensure safety.

**Validation with improved controllers.** In an additional experiment, we employed 15 controllers trained on a larger dataset. The results in Figure 8c show that under active learning, the average reward increased while the tolerance rate of FP decreased. This indicates that when paired with more trustworthy controllers, actively learned monitors correctly identify and have more confidence in the optimal controller, thus maximizing reward without reverting to the safety controller.

**Conclusion.** The active learning approach trains the model to be less conservative, enabling it to make more autonomous decisions rather than solely relying on the safety controller, particularly in situations where it is unable to make a clear judgment based on the current context. Conversely, the passively learned monitor loses basic "selection" functionality early on, and simply relies on the safety fallback to gain reward at the cost of high conservatism.

## 5.6 RQ4: Simplex vs multi-Simplex

This experiment aims to show the relationship between the false positive rates and the number of controllers. We train LR-based monitors on three sets of controllers taken from  $S_3$ . The sets have 1, 5, and 15 controllers, respectively. We do this for the three sets of controllers available in Section 5.4: the 15 controllers of Scenario 1 (Autonomous steering), and the two sets for Scenario 2 (Dynamic environment). We trained three monitors, one per set of controllers. The hyperparameters chosen were  $T = 1000$ ,  $e = 25$ , and  $n = 300$ , as

in Section 5.4. The monitors are evaluated over 500 simulations, generated using the same random seeds, for a fair comparison. Because the controllers of  $S_3$  are trained on diverse enough data, there is only a small difference between regarding their performance, and the reward is similar for the three sets as a consequence. Nevertheless, the reward grows with the number of controllers (see Figure 9a), and the set with 15 controllers has a reward that is 3% higher than the case with just one controller. However, it is important to notice that, **for the same confidence threshold, the false positives rate decreases significantly** with the number of controllers, since the confidence of the monitor on the best controller increases. Similar conclusions can be drawn from Figures 9b and 9c.

## 5.7 Monitoring computation overhead

Notice that the monitor selects a controller by multiplying the matrix of parameters  $\theta$  by the vector of contexts  $x$ , and then choosing the controller that outputs the minimum probability of violating the safety specification. For this reason, the computation overhead added by the monitor is minimal. Given a context, an LR-based monitor takes an average of  $4.51\mu s$  to select the controller. An NN-based monitor takes an average of  $204.61\mu s$  on CPU, although this computation could be accelerated using a GPU. The average was computed over 100 simulations.

## 6 CONCLUSION

We presented a new approach to learning safety monitors for ACPS based on contextual learning. Our approach utilizes methods from contextual bandits to learn monitors. Our results shows the significant impact of contextualizing monitors in selecting the right control and balancing safety and performance. Here we focused on positional contexts, based on static features. In the future, we plan to expand to state-based contexts, adapting both theory and algorithms.

## References

- [1] 2013. *Introduction to the Logistic Regression Model*. John Wiley & Sons, Ltd, Chapter 1, 1–33. arXiv:<https://onlinelibrary.wiley.com/doi/pdf/10.1002/9781118548387.ch1> doi:[10.1002/9781118548387.ch1](https://doi.org/10.1002/9781118548387.ch1)
- [2] Mohammed Alshiekh, Roderick Bloem, Rüdiger Ehlers, Bettina Könighofer, Scott Niekum, and Ufuk Topcu. 2018. Safe reinforcement learning via shielding. In *Proceedings of the Thirty-Second AAAI Conference on Artificial Intelligence and Thirtieth Innovative Applications of Artificial Intelligence Conference and Eighth AAAI Symposium on Educational Advances in Artificial Intelligence* (New Orleans, Louisiana, USA) (AAAI’18/IAAI’18/AAAI’18). AAAI Press, Article 326, 10 pages.
- [3] Dario Amodei, Chris Olah, Jacob Steinhardt, Paul Christiano, John Schulman, and Dan Mané. 2016. Concrete Problems in AI Safety. arXiv:[1606.06565](https://arxiv.org/abs/1606.06565) [cs.AI]
- [4] Ezio Bartocci, Jyotirmoy Deshmukh, Alexandre Donzé, Georgios Fainekos, Oded Maler, Dejan Někovič, and Sriram Sankaranarayanan. 2018. *Specification-Based Monitoring of Cyber-Physical Systems: A Survey on Theory, Tools and Applications*. Springer International Publishing, Cham, 135–175. doi:[10.1007/978-3-319-75632-5\\_5](https://doi.org/10.1007/978-3-319-75632-5_5)
- [5] Mariusz Bojarski, David W. del Testa, Daniel Dworakowski, Bernhard Firner, Beat Flepp, Prasoon Goyal, Lawrence D. Jackel, Mathew Monfort, Urs Muller, Jiakai Zhang, Xin Zhang, Jake Zhao, and Karol Zieba. 2016. End to End Learning for Self-Driving Cars. *ArXiv* abs/1604.07316 (2016). <https://api.semanticscholar.org/CorpusID:15780954>
- [6] Djallel Bouneffouf, Irina Rish, and Charu C. Aggarwal. 2020. Survey on Applications of Multi-Armed and Contextual Bandits. In *IEEE Congress on Evolutionary Computation, CEC 2020, Glasgow, United Kingdom, July 19–24, 2020*. IEEE, 1–8.
- [7] Emil Carlsson, Debabrota Basu, Fredrik D. Johansson, and Devdatt P. Dubhashi. 2024. Pure Exploration in Bandits with Linear Constraints. In *International Conference on Artificial Intelligence and Statistics, 2-4 May 2024, Palau de Congressos, Valencia, Spain (Proceedings of Machine Learning Research, Vol. 238)*, Sanjoy Dasgupta, Stephan Mandt, and Yingzhen Li (Eds.). PMLR, 334–342.
- [8] Chao Chen, Jie Liu, Chang Zhou, Jie Tang, and Gangshan Wu. 2024. Sketch and Refine: Towards Fast and Accurate Lane Detection. In *Thirty-Eighth AAAI Conference on Artificial Intelligence, AAAI 2024, Thirty-Sixth Conference on Innovative Applications of Artificial Intelligence, IAAI 2024, Fourteenth Symposium on Educational Advances in Artificial Intelligence, EAAI 2024, February 20–27, 2024, Vancouver, Canada*, Michael J. Wooldridge, Jennifer G. Dy, and Sriraam Natarajan (Eds.). AAAI Press, 1001–1009. doi:[10.1609/AAAI.V38I2.27860](https://doi.org/10.1609/AAAI.V38I2.27860)
- [9] Zhili Chen and Xinning Huang. 2017. End-to-end learning for lane keeping of self-driving cars. In *2017 IEEE Intelligent Vehicles Symposium (IV)*. 1856–1860. doi:[10.1109/IVS.2017.7995975](https://doi.org/10.1109/IVS.2017.7995975)
- [10] Nirjhar Das, Souradip Chakraborty, Aldo Pacchiano, and Sayak Ray Chowdhury. 2024. Active Preference Optimization for Sample Efficient RLHF. <https://api.semanticscholar.org/CorpusID:26774053>
- [11] Ankush Desai, Tommaso Dreossi, and Sanjit A. Seshia. 2017. Combining Model Checking and Runtime Verification for Safe Robotics. In *17th International Conference on Runtime Verification (RV)*. 172–189.
- [12] Alexey Dosovitskiy, German Ros, Felipe Codevilla, Antonio Lopez, and Vladlen Koltun. 2017. CARLA: An Open Urban Driving Simulator. In *Proceedings of the 1st Annual Conference on Robot Learning (Proceedings of Machine Learning Research, Vol. 78)*, Sergey Levine, Vincent Vanhoucke, and Ken Goldberg (Eds.). PMLR, 1–16. <https://proceedings.mlr.press/v78/dosovitskiy17a.html>
- [13] Louis Fauré, Marc Abeille, Clément Calauzénès, and Olivier Fercoq. 2020. Improved optimistic algorithms for logistic bandits. In *International Conference on Machine Learning*. PMLR, 3052–3060.
- [14] Louis Fauré, Marc Abeille, Kwang-Sung Jun, and Clément Calauzénès. 2022. Jointly Efficient and Optimal Algorithms for Logistic Bandits. In *International Conference on Artificial Intelligence and Statistics, AISTATS 2022, 28-30 March 2022, Virtual Event (Proceedings of Machine Learning Research, Vol. 151)*, Gustau Camps-Valls, Francisco J. R. Ruiz, and Isabel Valera (Eds.). PMLR, 546–580.
- [15] Sarah Filippi, Olivier Cappé, Aurélien Garivier, and Csaba Szepesvári. 2010. Parametric Bandits: The Generalized Linear Case. In *Advances in Neural Information Processing Systems 23: 24th Annual Conference on Neural Information Processing Systems 2010. Proceedings of a meeting held 6-9 December 2010, Vancouver, British Columbia, Canada*, John D. Lafferty, Christopher K. I. Williams, John Shawe-Taylor, Richard S. Zemel, and Aron Culotta (Eds.). Curran Associates, Inc., 586–594.
- [16] Bernd Finkbeiner and Henny Sipma. 2004. Checking Finite Traces Using Alternating Automata. *Form. Methods Syst. Des.* 24, 2 (March 2004), 101–127. doi:[10.1023/B:FORM.0000017718.28096.48](https://doi.org/10.1023/B:FORM.0000017718.28096.48)
- [17] Daniel J. Fremont, Johnathan Chiu, Dragos D. Margineantu, Denis Osipovych, and Sanjit A. Seshia. 2020. Formal Analysis and Redesign of a Neural Network-Based Aircraft Taxiing System with VeriFAI. In *Computer Aided Verification: 32nd International Conference, CAV 2020, Los Angeles, CA, USA, July 21–24, 2020, Proceedings, Part I* (Los Angeles, CA, USA). Springer-Verlag, Berlin,

Heidelberg, 122–134. [doi:10.1007/978-3-030-53288-8\\_6](https://doi.org/10.1007/978-3-030-53288-8_6)

[18] Daniel J. Fremont, Tommaso Dreossi, Shromona Ghosh, Xiangyu Yue, Alberto L. Sangiovanni-Vincentelli, and Sanjit A. Seshia. 2019. Scenic: a language for scenario specification and scene generation. In *Proceedings of the 40th ACM SIGPLAN Conference on Programming Language Design and Implementation* (Phoenix, AZ, USA) (PLDI 2019). Association for Computing Machinery, New York, NY, USA, 63–78. [doi:10.1145/3314221.3314633](https://doi.org/10.1145/3314221.3314633)

[19] Kai-Chieh Hsu, Haimin Hu, and Jaime F. Fisac. 2024. The Safety Filter: A Unified View of Safety-Critical Control in Autonomous Systems. *Annu. Rev. Control. Robotics Auton. Syst.* 7, 1 (2024). [doi:10.1146/ANNUREV-CONTROL-071723-102940](https://doi.org/10.1146/ANNUREV-CONTROL-071723-102940)

[20] Pushpak Jagtap, Sadegh Soudjani, and Majid Zamani. 2021. Formal Synthesis of Stochastic Systems via Control Barrier Certificates. *IEEE Trans. Automat. Control* 66, 7 (2021), 3097–3110. [doi:10.1109/TAC.2020.3013916](https://doi.org/10.1109/TAC.2020.3013916)

[21] Kyle D. Julian, Jessica Lopez, Jeffrey S. Brush, Michael P. Owen, and Mykel J. Kochenderfer. 2016. Policy compression for aircraft collision avoidance systems. In *2016 IEEE/AIAA 35th Digital Avionics Systems Conference (DASC)*. 1–10. [doi:10.1109/DASC.2016.7778091](https://doi.org/10.1109/DASC.2016.7778091)

[22] Andreas Kirsch and Yarin Gal. 2022. Unifying Approaches in Active Learning and Active Sampling via Fisher Information and Information-Theoretic Quantities. *Transactions on Machine Learning Research* (2022). Expert Certification.

[23] Branislav Kveton, Manzil Zaheer, Csaba Szepesvári, Lihong Li, Mohammad Ghavamzadeh, and Craig Boutilier. 2020. Randomized exploration in generalized linear bandits. In *International Conference on Artificial Intelligence and Statistics*. PMLR, 2066–2076.

[24] John Langford and Tong Zhang. 2007. The Epoch-Greedy Algorithm for Multi-armed Bandits with Side Information. In *Advances in Neural Information Processing Systems*, J. Platt, D. Koller, Y. Singer, and S. Roweis (Eds.), Vol. 20. Curran Associates, Inc. [https://proceedings.neurips.cc/paper\\_files/paper/2007/file/4b04a686b0ad13dce35fa99fa4161c65-Paper.pdf](https://proceedings.neurips.cc/paper_files/paper/2007/file/4b04a686b0ad13dce35fa99fa4161c65-Paper.pdf)

[25] Tor Lattimore and Csaba Szepesvári. 2020. *Bandit algorithms*. Cambridge University Press.

[26] Junghyun Lee, Se-Young Yun, and Kwang-Sung Jun. 2024. Improved Regret Bounds of (Multinomial) Logistic Bandits via Regret-to-Confidence-Set Conversion. In *International Conference on Artificial Intelligence and Statistics, 2-4 May 2024, Palau de Congressos, Valencia, Spain (Proceedings of Machine Learning Research, Vol. 238)*. Sanjoy Dasgupta, Stephan Mandt, and Yingzhen Li (Eds.). PMLR, 4474–4482. <https://proceedings.mlr.press/v238/lee24c.html>

[27] Xiao Li, H. Eric Tseng, Anouck Girard, and Ilya Kolmanovsky. 2024. Autonomous Driving With Perception Uncertainties: Deep-Ensemble Based Adaptive Cruise Control. In *2024 IEEE 63rd Conference on Decision and Control (CDC)*. 8186–8192. [doi:10.1109/CDC56724.2024.10886150](https://doi.org/10.1109/CDC56724.2024.10886150)

[28] Oded Maler and Dejan Nickovic. 2004. Monitoring Temporal Properties of Continuous Signals. In *Formal Techniques, Modelling and Analysis of Timed and Fault-Tolerant Systems, Joint International Conference on Formal Modelling and Analysis of Timed Systems, FORMATS 2004 and Formal Techniques in Real-Time and Fault-Tolerant Systems, FTRTFT 2004, Grenoble, France, September 22-24, 2004, Proceedings (Lecture Notes in Computer Science, Vol. 3253)*, Yassine Lakhnech and Sergio Yovine (Eds.). Springer, 152–166. [doi:10.1007/978-3-540-30206-3\\_12](https://doi.org/10.1007/978-3-540-30206-3_12)

[29] Swapnil Mallick, Shuvam Ghosal, Anand Balakrishnan, and Jyotirmoy Deshmukh. 2023. Safety Monitoring for Pedestrian Detection in Adverse Conditions. In *Runtime Verification - 23rd International Conference, RV 2023, Thessaloniki, Greece, October 3-6, 2023, Proceedings (Lecture Notes in Computer Science, Vol. 14245)*. Panagiotis Katsaros and Laura Nenzi (Eds.). Springer, 389–399. [doi:10.1007/978-3-031-44267-4\\_22](https://doi.org/10.1007/978-3-031-44267-4_22)

[30] Stefan Mitsch and André Platzer. 2016. ModelPlex: verified runtime validation of verified cyber-physical system models. *Formal Methods Syst. Des.* 49, 1-2 (2016), 33–74. [doi:10.1007/s10703-016-0241-z](https://doi.org/10.1007/s10703-016-0241-z)

[31] Ioanna Mitsioni, Pouria Tajvar, Danica Kragic, Jana Tumova, and Christian Pek. 2023. Safe Data-Driven Model Predictive Control of Systems With Complex Dynamics. *IEEE Transactions on Robotics* 39, 4 (2023), 3242–3258. [doi:10.1109/TRO.2023.3266995](https://doi.org/10.1109/TRO.2023.3266995)

[32] Eshed Ohn-Bar, Aditya Prakash, Aseem Behl, Kashyap Chitta, and Andreas Geiger. 2020. Learning Situational Driving. In *2020 IEEE/CVF Conference on Computer Vision and Pattern Recognition (CVPR)*. 11293–11302. [doi:10.1109/CVPR42600.2020.01131](https://doi.org/10.1109/CVPR42600.2020.01131)

[33] Shreyas Ramakrishna, Charles Harstell, Matthew P. Burruss, Gabor Karsai, and Abhishek Dubey. 2020. Dynamic-weighted simplex strategy for learning enabled cyber physical systems. *Journal of Systems Architecture* 111 (2020), 101760. [doi:10.1016/j.sysarc.2020.101760](https://doi.org/10.1016/j.sysarc.2020.101760)

[34] Carlos Riquelme, George Tucker, and Jasper Snoek. 2018. Deep bayesian bandits showdown: An empirical comparison of bayesian deep networks for thompson sampling. *arXiv preprint arXiv:1802.09127* (2018).

[35] SAE J3016. 2014. On-Road Automated Vehicle Standards Committee. Taxonomy and definitions for terms related to on-road motor vehicle automated driving systems. <https://cir.nii.ac.jp/crid/1370861704794099599>

[36] Sanjit A. Seshia, Dorsa Sadigh, and S. Shankar Sastry. 2016. Towards Verified Artificial Intelligence. *ArXiv e-prints* (July 2016). arXiv:1606.08514

[37] Lui Sha. 2001. Using simplicity to control complexity. *IEEE Software* 18, 4 (July 2001), 20–28. [doi:10.1109/MS.2001.936213](https://doi.org/10.1109/MS.2001.936213)

[38] Jack Sherman and Winifred J. Morrison. 1950. Adjustment of an Inverse Matrix Corresponding to a Change in One Element of a Given Matrix. *The Annals of Mathematical Statistics* 21, 1 (1950), 124–127. <http://www.jstor.org/stable/2236561>

[39] Junbo Tong, Shuhan Du, and Wenhui Fan. 2025. Ensemble Neural Network-Based Approximate Model Predictive Control With Strict Guarantees. *International Journal of Robust and Nonlinear Control* 35 (2025), 7295 – 7308. <https://api.semanticscholar.org/CorpusID:279931246>

[40] Pan Xu, Zheng Wen, Handong Zhao, and Quanquan Gu. 2020. Neural contextual bandits with deep representation and shallow exploration. *arXiv preprint arXiv:2012.01780* (2020).

[41] Beyazit Yalcinkaya, Hazem Torfah, Ankush Desai, and Sanjit A. Seshia. 2023. Ulgen: A Runtime Assurance Framework for Programming Safe Cyber-Physical Systems. *IEEE Transactions on Computer-Aided Design of Integrated Circuits and Systems* 42, 11 (2023), 3679–3692. [doi:10.1109/TCAD.2023.3246386](https://doi.org/10.1109/TCAD.2023.3246386)

[42] Luyao Zhang, Georgios Pantazis, Shaohang Han, and Sergio Grammatico. 2024. An Efficient Risk-aware Branch MPC for Automated Driving that is Robust to Uncertain Vehicle Behaviors. In *2024 IEEE 63rd Conference on Decision and Control (CDC)*. 8207–8212. [doi:10.1109/CDC56724.2024.10886383](https://doi.org/10.1109/CDC56724.2024.10886383)

[43] Amirhossein Zolfagharian, Manel Abdellatif, Lionel C. Briand, and Ramesh S. 2025. SMARLA: A Safety Monitoring Approach for Deep Reinforcement Learning Agents. *IEEE Transactions on Software Engineering* 51, 01 (Jan. 2025), 82–105. [doi:10.1109/TSE.2024.3491496](https://doi.org/10.1109/TSE.2024.3491496)

## Appendix Outline

In this appendix, we extend some results of our paper.

- We provide details on how the epistemic uncertainty is computed in line 6 of Algorithm 1.
- We provide a complete proof for Theorem 4.1.
- We provide additional details of the experiments performed.
- We include a plot illustrating the behavior of the monitoring policy in one simulation run.
- We include the SCENIC program used to generate scenes for simulations.

## A Epistemic Uncertainty

The key component of our approach is how to decide which controller to test during the learning phase. At every time  $t$ , the learner keeps track of the current MLE estimate of each controller,  $\theta_{t,c}$ ,

$$\theta_{t,c} \in \operatorname{argmax}_{\theta} \sum_{j=1}^t \mathbb{1}_{(C_j=c)} (Y_j \log \sigma(\theta_c^\top \xi_j) + (1 - Y_j) \log(1 - \sigma(\theta_c^\top \xi_j)))$$

and the corresponding Hessian of the negative log-likelihood

$$\mathbf{H}_t(\theta_{c,t}) = \sum_{s=1}^t \mathbf{I}_{(C_s=c)} \dot{\sigma}(\theta_{c,t}^\top \xi_s) \xi_s \xi_s^\top \quad (1)$$

where  $\xi_s$  is the context observed in round  $s$ , and  $\dot{\sigma}(\cdot) = \sigma(\cdot)(1 - \sigma(\cdot))$  is the derivative of  $\sigma(\cdot)$ . Intuitively, the Hessian indicates the curvature while moving in a particular direction. A higher curvature indicates more sensitivity to changes in that direction, which is linked to more uncertainty because small changes lead to unpredictable results.

At each round, we choose to test a controller and a context that satisfy

$$C_t \in \operatorname{argmax}_{c \in C} \|\xi_{t+1}\|_{H_t^{-1}(\theta_{c,t})} \quad \xi_t \in \operatorname{argmax}_{\xi \in \mathbb{D}^{V_{\text{cont}}}} \|\xi\|_{H_t^{-1}(\theta_{C_t,t})} \quad (2)$$

where  $\|x\|_V = |\sqrt{x^\top V x}|$ . The quantity  $\|\xi_{t+1}\|_{H_t^{-1}(\theta_{c,t})}$  measures our epistemic uncertainty about the performance of controller  $c$  in the direction of the vector  $\xi_{t+1}$  (see [10, 22]) and sampling criterion in Equation (2) will output a controller and a context with the highest epistemic uncertainty.

The Hessian is updated using the Sherman-Morrison formula [38]. The intuition behind using this formula is that it efficiently computes the inverse of a matrix that has been modified by just a rank-one update. This formula provides :

$$H_t^{-1}(\theta_{t-1}) = H_{t-1}^{-1}(\theta_{t-1}) - \frac{H_{t-1}^{-1}(\theta_{t-1}) \xi_t \xi_t^\top H_{t-1}^{-1}(\theta_{t-1})}{1 + \dot{\sigma}(\xi_t^\top \theta_{t-1}) \|\xi_t\|_{H_{t-1}^{-1}(\theta_{t-1})}^2}$$

## B Proof of Theorem 1

Notice that our goal is to learn an optimal policy  $\pi$  such that it minimizes the regret:

$$\max_{\xi \in \mathbb{D}^{V_{\text{cont}}}} |\sigma(\theta_{\pi(\xi)}^\top \xi) - \sigma(\theta_{\pi^*(\xi)}^\top \xi)|$$

where  $\pi(\xi) \in \operatorname{argmin}_{c \in C} \sigma(\theta_c^\top \xi)$

This is, we want to find the vectors  $\{\theta_c\}_{c \in C}$  that solve the minimization problem above.

To derive theoretical bounds on the regret of our problem, we first derive bounds for a more complex problem and then use them to bound the regret. We start by showing how to use padding to transform the previous problem into the problem of minimizing the regret for every controller, and not just for the safest one. This is, not only for the one that minimizes  $\sigma(\theta_c^\top \xi)$ .

After this transformation, we can apply Theorems B.1 and B.2 of the following sections to prove Theorem 4.1.

### B.1 Conversion using padding

Let  $\xi \in \mathbb{D}^{V_{\text{cont}}} (\subset \mathbb{R}^d)$  a context and  $n = |C|$  the number of controllers. For each controller  $c_i \in C$  with  $1 \leq i \leq n$  we define  $\xi^i \in \mathbb{R}^{n \cdot d}$  as follows:

$$(\xi^i)_j = \begin{cases} (\xi)_{j-(i-1)d} & \text{if } (i-1)d + 1 \leq j \leq id \\ 0 & \text{otherwise} \end{cases}$$

Notice that, to generate vectors  $\xi^i$ , we strategically add 0-padding to the context vector  $\xi$ , and that computing the maximum likelihood estimate is equivalent to computing:

$$\theta_{T,c} \in \operatorname{argmax}_{\theta} \sum_{t=1}^T \mathbb{1}_{(C_t=c)} (Y_t \log \sigma(\theta^\top \xi_t^i) + (1 - Y_t) \log(1 - \sigma(\theta^\top \xi_t^i)))$$

At each step of Algorithm 1 we can define the data point  $\{\xi_t^i, Y_t\}$  where  $c_i = C_t$ . We can define  $\theta_T \in \mathbb{R}^{n \cdot d}$  such that its values between positions  $(i-1)d + 1$  and  $id$  correspond to  $\theta_{T,c_i}$ . Because of the definition of  $\xi^i$ , computing  $\theta_{T,c}$  for every controller  $c$  is equivalent to compute:

$$\theta_T \in \operatorname{argmax}_{\theta} \sum_{t=1}^T (Y_t \log \sigma(\theta^\top \xi_t^i) + (1 - Y_t) \log(1 - \sigma(\theta^\top \xi_t^i))) \quad (3)$$

Assuming that  $\theta_{T^*}$  converges to the optimal policy  $\pi$  for a sufficiently large value  $T^*$ , the regret of our problem is then equivalent to:

$$R := \max_{\xi \in \mathbb{D}^{V_{\text{cont}}}} |\sigma(\theta_*^\top \xi^m) - \sigma(\theta_{T^*}^\top \xi^m)|$$

where  $c_m \in \operatorname{argmin}_{c \in C} \sigma(\theta_c^\top \xi)$

We define now the following regret:

$$R(T) := \max_{\substack{\xi \in \mathbb{D}^{V_{\text{cont}}} \\ 1 \leq i \leq n}} |\sigma(\theta_*^\top \xi^i) - \sigma(\theta_T^\top \xi^i)| < \max_{\substack{\xi \in \mathbb{D}^{V_{\text{cont}}} \\ 1 \leq i \leq n}} |\theta_*^\top \xi^i - \theta_T^\top \xi^i|$$

Where the inequality comes from  $\sigma(\cdot)$  being Lipschitz with constant  $1/4$ .

It is clear that  $R \leq R(T^*)$ . It remains to show that  $R(T)$  conforms with the bounds as stated in Theorem 4.1.

## B.2 Results needed to prove Theorem 4.1

For each iteration of the bandits' algorithm, there is a bound on the error between the optimal monitor and the learned monitor. This is a consequence of Lemma 1 of [10].

LEMMA B.1 (ESTIMATION ERROR AT ROUND  $t$  [10]). *Let  $\delta \in (0, 1]$ . Assuming that the optimal monitor is bounded, i.e.,  $\|\theta_*\| \leq q$  for some  $q > 0$ , let  $\lambda = \frac{1}{4q^2(2+q)^2}$ . Then, using Algorithm 1 to train a monitor  $\theta_t \in \mathbb{R}^{n \cdot d}$  at each round  $t$ , with probability at least  $1 - \delta$ , we have for some constant  $b > 0$ ,*

$$\|\theta_* - \theta_t\|_{H_t(\theta_t)} \leq bq^{1/2}\gamma_t(\delta) \quad (4)$$

with  $\gamma_t(\delta) = bq\sqrt{nd \log \frac{qT}{nd} + \log \frac{t}{\delta}}$ ,  $\|\theta_*\|$  the Euclidean norm of  $\theta_*$ , and  $H_t(\theta_t)$  the Hessian as defined in Equation (1).

The details of the proof can be found in [10].

The next Lemma allows us to derive the final bound of Theorem 4.1, as can be seen in the next section.

LEMMA B.2 (ELLIPTIC POTENTIAL LEMMA [25]). *Let  $\{x_s\}_{s=1}^t$  be a sequence of vectors in  $\mathbb{R}^d$  such that  $\|x_s\| \leq L < \infty$  for any  $s \in [t]$ . Let  $V_t = \sum_{s=1}^{t-1} x_s x_s^\top + \lambda I$ . Then,*

$$\sum_{s=1}^t \|x_s\|_{V_s^{-1}}^2 \leq 2d \log \left(1 + \frac{tL^2}{\lambda d}\right)$$

## B.3 Proof of Theorem 4.1

We start with a reminder of Theorem 1:

*Using Algorithm 1, selecting the controller and context with the highest uncertainty, we have that the regret decays with the number of rounds  $T$  with order  $O(\sqrt{\log(T)^2/T})$ .*

In order to prove Theorem 4.1, we show that the following suboptimality gap  $R(T, x) := \|\theta_*^\top x - \theta_T^\top x\|$  is bounded for every (padded) context  $x$ . This is important because, by definition,  $R(T) \leq \max_x R(T, x)$ .

We show that  $R(T, x)$  is bounded in terms of  $\|\theta_* - \theta_t\|_{H_t^{-1}(\theta_t)}$  and in terms of  $\|x\|_{H_t^{-1}(\theta_t)}$ , the uncertainty of the context. This allows us to apply Theorems B.1 and B.2 to find bounds of  $R(T, x)$  in terms of  $T$ .

Before proving Theorem 4.1, it is necessary to prove the following corollary, which follows from Theorem B.1.

COROLLARY B.3. *Let  $\delta \in (0, 1]$ . With probability at least  $1 - \delta$ , Algorithm 1 holds the following bound:*

$$R(T) \leq b\gamma_T(\delta)\sqrt{q \log\left(1 + \frac{T}{\lambda\kappa nd}\right) \frac{\kappa nd}{T}}$$

for a constant  $b > 0$ ,  $\gamma_t(\delta)$ ,  $q$  and  $\lambda$  as defined in Theorem B.1, and  $\kappa = \max_{x \in \mathcal{X}} \max_{\theta \in \Theta} \frac{1}{\sigma(\theta^\top x)}$ .

In the experiments, we use the MLE (Equation (3)) to estimate the policy  $\pi$ . For the proof of Theorem B.3, we use  $\theta_T = \frac{1}{T} \sum_{t=1}^T \theta_t$  to get the bounds on  $R(T, x)$ . This average of the MLE estimators quickly converges to the MLE for sufficiently large values of  $T$ , and will help us derive the theoretical bounds.

For a (padded) context  $x \in \mathbb{R}^{n \cdot d}$ , we have that:

$$\begin{aligned} R(T, x) &= \|\theta_*^\top x - \theta_T^\top x\| = \|(\theta_*^\top - \frac{1}{T} \sum_{t=1}^T \theta_t^\top)x\| \\ &\leq \frac{1}{T} \sum_{t=1}^T \|(\theta_*^\top - \theta_t^\top)x\| \\ &\quad (\text{Cauchy-Schwarz}) \\ &\leq \frac{1}{T} \sum_{t=1}^T \|\theta_*^\top - \theta_t^\top\|_{H_t(\theta_t)} \|x\|_{H_t^{-1}(\theta_t)} \\ &\quad (\text{Theorem B.1}) \\ &\leq \frac{bq^{1/2}\gamma_T(\delta)}{T} \sum_{t=1}^T \|x\|_{H_t^{-1}(\theta_t)} \\ &\leq \frac{bq^{1/2}\gamma_T(\delta)}{T} \sum_{t=1}^T \|x_t\|_{H_t^{-1}(\theta_t)} \end{aligned}$$

We use that  $x_t \in \operatorname{argmax}_{x \in \mathcal{X}} \|x\|_{H_t^{-1}(\theta_t)}$  to get the last inequality, this is,  $x_t$  is the context with the highest uncertainty.

Now, because  $V_t \preceq \kappa H_t(\theta_t)$ , we have that we can upper bound  $\|x_t\|_{H_t^{-1}(\theta_t)}$  by  $\sqrt{\kappa} \|x_t\|_{V_t^{-1}}$ . For this reason, we can apply Theorem B.2. Then,

$$\begin{aligned} R(T, x) &\leq \frac{b\sqrt{\kappa q}\gamma_T(\delta)}{T} \sum_{t=1}^T \|x_t\|_{V_t^{-1}} \\ &\quad (\text{Cauchy-Schwarz}) \\ &\leq \frac{b\sqrt{\kappa q}\gamma_T(\delta)}{T} \sqrt{T \sum_{t=1}^T \|x_t\|_{V_t^{-1}}^2} \\ &\quad (\text{Theorem B.2}) \\ &\leq \frac{b\sqrt{\kappa q}\gamma_T(\delta)}{T} \sqrt{2ndT \log\left(1 + \frac{T}{\lambda\kappa nd}\right)} \\ &\quad (\text{Def. of } \gamma_T(\delta)) \\ &= bq^{3/2} \sqrt{\left(nd \log\left(\frac{qT}{nd}\right) + \log\left(\frac{T}{\delta}\right)\right)} \cdot \\ &\quad \sqrt{\log\left(1 + \frac{T}{\lambda\kappa nd}\right) \frac{\kappa nd}{T}} \end{aligned}$$

Finally, because  $R(T) \leq \max_x R(T, x)$ , and seeing that in the last inequality  $b, q, n, d, \delta, \lambda$ , and  $\kappa$  are constants, we can deduce Theorem 4.1.

## C Experiments

In this section, we explain the missing details related to the experiments, and we include an example of a simulation, where we show how the monitor works in practice.

### C.1 CNN Structure

The CNN controllers have the structure shown in Figure 12: three convolutional layers, with two fully connected layers at the end. Depending on the scenario, the output will be given by  $N = 1$  (CTE) or  $N = 2$  neurons (CTE, target speed).

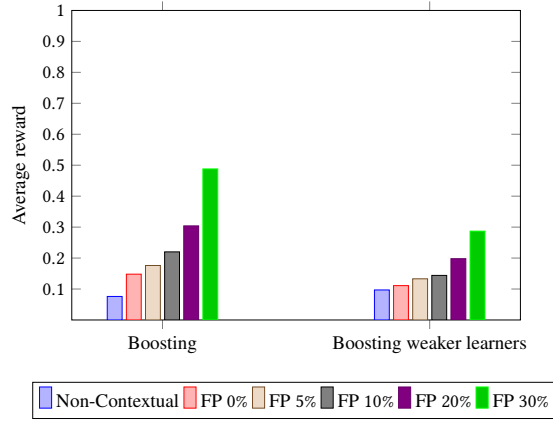


Figure 10: Extension of RQ2: Contextual vs. Boosting

## C.2 Controllers of Experiment Contextual vs Bagging

The 15 biased controllers are trained each on a specific context  $\xi = (w, t, i, d)$  such that  $(w, t)$  is given by one of the weather presets  $W = \{ClearNoon, ClearSunset, HardRainNoon, HardRainSunset, CloudyNoon\}$ , and  $d$  take values of  $d = 100$  (no other car ahead),  $d \in [5, 10]$ , or  $d \in [20, 30]$ .

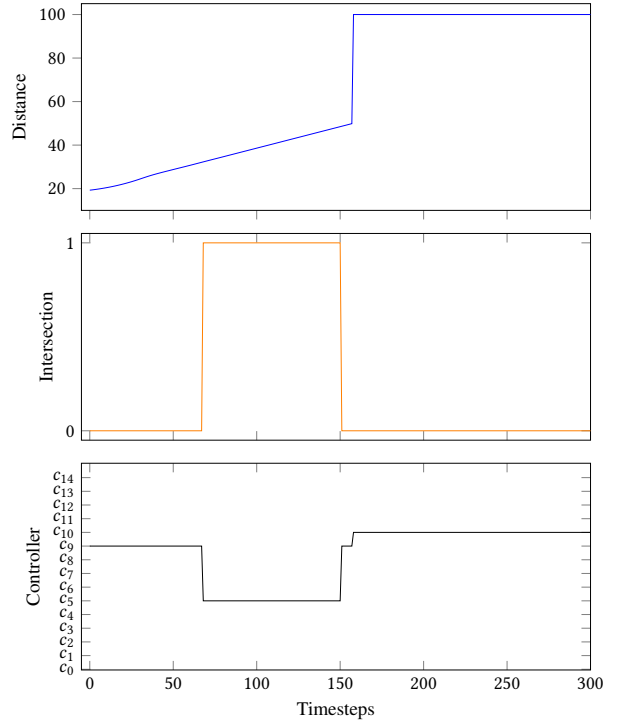
## C.3 Contextual vs. Boosting

We further used adaptive boosting to train an ensemble of 15 controllers for Scenario 1. This ensemble did not perform well, achieving much worse performance than any other model. The main reason is that the first controller trained learns with high accuracy, and the rest overfit on the few data points for which the first is poor. As a consequence, 14 out of 15 controllers do not generalize well, and the performance of the first controller is diluted due to the influence of the others (see Figure 10). We evaluated a second boosting ensemble using weaker learners on 100 simulations and obtained similar results. For these reasons, we decided not to use them as baselines.

We designed another boosting ensemble using weaker learners, specifically using smaller CNNs. The goal was to determine whether the controllers would overfit even when using weaker learners that would perform worse individually. The results indicate that the models still overfit, and because the controllers are now less complex, the performance of the monitor is worse.

## C.4 Example behavior of monitor along a simulation

In Figure 11, we use one of the testing simulations to illustrate how our monitors work. The weather during this simulation is *WetNoon*. We can observe that, at the beginning, the ego car is on a straight road (intersection=0) with another car around 20 meters ahead (distance=20). The ego car uses first the controller  $c_9$ . Once it arrives at an intersection, after around 60 time steps, it switches to the controller  $c_5$ . Finally, shortly after leaving the intersection, the ego car stops seeing the car ahead, represented by distance=100. The monitor switches momentarily to the controller  $c_9$  before switching to the controller  $c_{10}$  after leaving the intersection.

Figure 11: Example of a simulation, where a monitor of Use Case 1 and Setting  $S_3$  (Figure 7c) switches between controllers based on the weather, the distance to a car ahead, and the road type.

During the simulation, the lowest confidence of the monitor on one of the controllers is 0.9783. If we had used a confidence threshold higher than that value, the monitor would have switched to the safe controller instead.

## D Scenic Program

The SCENIC program of Figure 13 creates scenes for simulations where there is another car ahead of the ego car. The program generates a scene choosing one of the 14 weather presets available in CARLA. Then, it places the ego car in the center of a random lane. Finally, it places another car in front of the ego car with a random distance between 5 and 50. The cars will then drive at constant speed. The monitor is incorporated in the behavior of the ego car: EgoBehavior.

```
class convNet(torch.nn.Module):
    def __init__(self):
        super(convNet, self).__init__()

        self.model = torch.nn.Sequential(
            torch.nn.Conv2d(3, 32, kernel_size=3, stride=2),
            torch.nn.LeakyReLU(),
            torch.nn.MaxPool2d(kernel_size=2),
            torch.nn.Conv2d(32, 64, kernel_size=3, stride=2),
            torch.nn.LeakyReLU(),
            torch.nn.MaxPool2d(kernel_size=2),
            torch.nn.Conv2d(64, 128, kernel_size=3, stride=2),
            torch.nn.Flatten(),

            self.fc1 = torch.nn.Linear(1025, 1024)
            self.head = torch.nn.Linear(1024, N)
        )
```

**Figure 12: Definition of the CNNs used as controllers.**

```

## SET MAP AND MODEL
param map = localPath('maps/Town01.xodr')
param carla_map = 'Town01'

## CONSTANTS
EGO_MODEL = "vehicle.tesla.model3"
EGO_SPEED = 5
CAR1_SPEED = Range(3, 7)
DIST_CAR1 = Range(5, 50)

## STATIC FEATURES
param weather = Uniform('ClearNoon', 'CloudyNoon', 'WetNoon',
    'WetCloudyNoon', 'MidRainyNoon', 'HardRainNoon', 'SoftRainNoon',
    'ClearSunset', 'CloudySunset', 'WetSunset', 'WetCloudySunset',
    'MidRainSunset', 'HardRainSunset', 'SoftRainSunset')

## DEFINING BEHAVIORS
behavior EgoBehavior(speed=10):
    action = LaneKSimplex("simulation_data")
    take action
    while True:
        try:
            take action
        interrupt when self.distanceToClosest(Object) < 6:
            take SetBrakeAction(1), SetThrottleAction(0)

## DEFINING SPATIAL RELATIONS

lane = Uniform(*network.lanes)
start = new OrientedPoint on lane.centerline
ego = new SimplexCarlaCar at start,
    with blueprint EGO_MODEL,
    with behavior EgoBehavior(EGO_SPEED))

car1 = new Car following roadDirection from start for DIST_CAR1,
    with behavior FollowLaneBehavior(CAR1_SPEED)

require ego can see car1

terminate when ego.collision > 0 and ego.speed < 0.1
    and (distance to start) > 1

```

**Figure 13: Example of SCENIC program for Use Case 1: Lane Keeping.**

```

ego = new SimplexCarlaCar at start,
  with model_path globalParameters.controller_path,
  with blueprint EGO_MODEL,
  with behavior EgoBehavior(EGO_SPEED), # EgoBehavior(EGO_SPEED),
  # with logger CarlaLogger(f"{global_folder}/modd_{current_modd}/simulation_data")
  with logger CarlaLogger(f"{globalParameters.global_folder}/modd_{current_modd}/simulation_data")

for i in range(5):
    random_spot = new OrientedPoint following roadDirection from start for
        Range(DIST_PEDESTRIAN-1, DIST_PEDESTRIAN+50)

    side_offset = 8 # Range(1,8) # Distance from road center
    side_direction = Discrete({1: 0.5, -1: 0.5}) # Left or right side randomly

    p = new Pedestrian right of random_spot by side_direction * side_offset,
        with heading side_direction * 90 deg relative to random_spot.heading,
        with regionContainedIn None,
        with behavior CrossRoadBehavior(PEDESTRIAN_MIN_SPEED, THRESHOLD)

    PEDESTRIANS += [p]

for i in range(5):
    random_spot = new OrientedPoint following roadDirection from start for
        Range(DIST_CAR1-1, DIST_CAR1+50)
    side_movement = Discrete({0: 0.5, 3: 0.5}) # Left lane or same lane

    start_spot = new OrientedPoint left of random_spot by side_movement

    car1 = new Car following roadDirection from start_spot for Range(-1, 1),
        with behavior KeepDistance(CAR1_SPEED)

    CARS += [car1]

```

**Figure 14: Fragment of SCENIC program for Use Case 2: Collision Avoidance.**